JCTC Journal of Chemical Theory and Computation

Article

pubs.acs.org/JCTC

Effect of Dot Size on Exciton Binding Energy and Electron−Hole Recombination Probability in CdSe Quantum Dots

Jennifer M. Elward and Arindam Chakraborty*

Department of Chemistry, Syracuse University, Syracuse, New York 13244, United States

ABSTRACT: Exciton binding energy and electron−hole recombination probability are presented as two important metrics for investigating effect of dot size on electron−hole interaction in CdSe quantum dots. Direct computation of electron−hole recombination probability is challenging because it requires an accurate mathematical description of the electron−hole wave function in the neighborhood of the electron−hole coalescence point. In this work, we address this challenge by solving the electron−hole Schrodinger equation using the electron−hole explicitly correlated Hartree−Fock (eh-XCHF) method. The calculations were performed for a series of CdSe clusters ranging from $Cd_{20}Se_{19}$ to $Cd_{74608}Se_{74837}$ that correspond to dot diameter range 1−20 nm. The calculated exciton binding energies and electron−hole recombination probabilities were found to decrease with increasing dot size. Both of these quantities were found to scale as D_{dot}^{-n} with respect to the dot diameter D. One of the key insights from this study is that the electron−hole recombination probability decreases at a much faster rate than the exciton binding energy as a function of dot size. It was found that an increase in the dot size by a factor of 16.1, resulted in a decrease in the exciton binding energy and electron−hole recombination probability by a factor of 12.9 and 4.55×10^5, respectively.

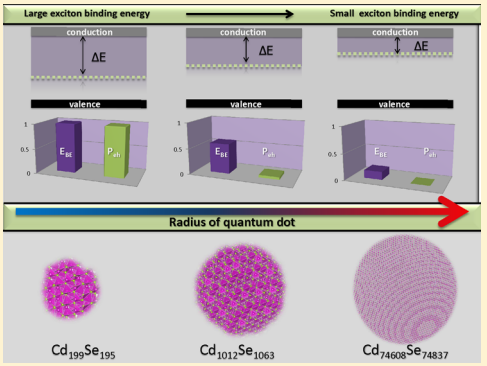

1. INTRODUCTION

Semiconductor quantum dots and rods have been the focus of intense theoretical and experimental research because of inherent size-dependent optical and electronic properties. Generation of bound electron−hole pairs (excitons) and their subsequent dissociation into free charge carriers are the two important factors that directly impact the light-harvesting efficiency of the semiconductor quantum dots. The dissociation of excitons is a complex process that is influenced by various factors such as shape and size of the quantum dots,[1−6] presence of surface defects,[7−9] surface ligands,[10,11] and coupling with phonon modes.[12−19] The energetics of the electron−hole interaction in quantum dots is quantified by the exciton dissociation energy and has been determined using both theoretical and experimental techniques.[20−22] Generation of free charge carriers by exciton dissociation has been facilitated by introducing core/shell heterojunctions[23−25] and applying external and ligand-induced electric fields.[26−31]

One of the direct routes for enhancing exciton dissociation is by modifying the size and shape of quantum dots. Studies on CdSe and other quantum dots have shown that the exciton binding energy decreases with increasing dot size.[32−40] The size of the quantum dots also has significant impact on the Auger recombination,[41,42] multiple exciton generation,[4,43−45] and blinking effect in quantum dots.[2,3,46] In addition to exciton binding energy, the spatial distribution of electrons and holes in quantum dots also provides important insight into the exciton dissociation process.[47,48] Electron and hole densities $\rho_e(r)$ and $\rho_h(r)$ have been widely used to investigate quasi-particle distribution in quantum dots.[23,24] For example in core/shell quantum dots, presence of the heterojunction induces asymmetric spatial distribution of electrons and holes, which, in turn, facilitates the exciton dissociation. Asymmetric electron probability density in the shell region of the core/shell quantum dots has been attributed to fast electron transfer from the quantum dots.[23,24,49,50]

The central challenge in the theoretical investigation of quantum dots is efficient computational treatment of large number of electrons in the system. For small clusters where all-electron treatment is feasible, ground state and excited-state calculations have been performed using GW Bethe-Salpeter,[51−53] density functional theory (DFT),[54−60] time-dependent DFT (TDDFT),[61−68] and MP2.[69] For bigger quantum dots where all-electron treatment is computationally prohibitive, atomistic semiempirical pseudopotential methods have been used extensively.[32,37,42,70,71] In this approach, the one-particle Schrödinger equation incorporating the pseudopotential v_{ps}

$$\left[-\frac{\hbar^2}{2m}\nabla^2 + v_{ps}\right]\phi_i = \lambda_i\phi_i \tag{1}$$

is solved and the eigenfunctions are used in construction of the quasiparticle states.[32,37] The quasiparticle states serve as a basis for both configuration interaction (CI) and perturbation theory calculations. Solution of eq 1 is generally obtained by introducing a set of basis functions (typically plane-waves), constructing the Hamiltonian matrix in that basis, and

Received: June 9, 2013
Published: September 5, 2013

diagonalizing it. The computational efficiency of CI has been greatly improved by using only states near the band gap for construction of the CI space.[37,72] This technique alleviates the need to compute the entire eigenspectrum of the Hamiltonian matrix; however, successful implementation of this approach requires computation of selected eigenvalues and eigenfunctions of the Hamiltonian matrix. Computation of the specific eigenvalues of large matrices is challenging and various methods such as the folded-spectrum method,[73,74] filter-diagonalization method,[69,75] and generalized Davidson method[76,77] have been specifically developed to address this problem.

The main goal of this article is to compare the effect of dot size on exciton binding energy and electron−hole recombination probability. The central quantity of interest for the present work is the electron−hole pair density $\rho_{eh}(\mathbf{r}_e,\mathbf{r}_h)$. The electron−hole pair density is defined as the probability density of finding an electron and a hole in the neighborhood of $\mathbf{r}_e$ and $\mathbf{r}_h$, respectively. The pair density is a mathematically complicated quantity and is generally obtained from an underlying wave function. Direct construction of the pair-density is also possible as long as N-representability can be enforced.[78] For an interacting electron−hole system, the pair density is not equal to the product of electron and hole densities

$$\rho_{eh}(\mathbf{r}_e, \mathbf{r}_h) \neq \rho_e(\mathbf{r}_e)\rho_h(\mathbf{r}_h) \tag{2}$$

Furthermore, the electron−hole pair density contains information about the correlated spatial distribution of the electrons and hole that cannot be obtained from the product of individual electron and hole densities. Both electron−hole recombination probability and exciton binding energy can be computed from the pair density. The electron−hole interaction energy V_{eh} is the major component of the exciton binding energy and can be calculated from the electron−hole pair density using the following expression,

$$V_{eh} = \int d\mathbf{r}_e\, d\mathbf{r}_h \rho_{eh}(\mathbf{r}_e, \mathbf{r}_h) r_{eh}^{-1} \varepsilon^{-1}(\mathbf{r}_e, \mathbf{r}_h) \tag{3}$$

where, $\varepsilon^{-1}(\mathbf{r}_e,\mathbf{r}_h)$ is the inverse dielectric function. The electron−hole recombination probability, P_{eh}, is related to the pair density as

$$P_{eh} = \frac{1}{N_e N_h} \int d\mathbf{r}_e \int_{\mathbf{r}_e-\Delta/2}^{\mathbf{r}_e+\Delta/2} d\mathbf{r}_h \rho_{eh}(\mathbf{r}_e, \mathbf{r}_h) \tag{4}$$

where N_e and N_h are number of electrons and holes, respectively. In eq 4, we define electron−hole recombination probability as the probability of finding a hole in a cube of volume Δ^3 centered at the electron position. The computation of the recombination probability is especially demanding because it requires evaluation of the pair density at small interparticle distances. As a consequence, the form of the electron−hole wave function near the electron−hole coalescence point is very important.[79−84] In the present work, we address this challenge by using the electron−hole explicitly correlated Hartree−Fock (eh-XCHF) method.[79,80] The eh-XCHF method is a variational method where the wave function depends explicitly on the electron−hole interparticle distance and has been used successfully for investigating electron−hole interaction.[30,79,80]

The remainder of the article is organized as follows. The theoretical details of the eh-XCHF and its computational implementation for CdSe quantum dots are presented in sections 2 and 3, respectively. The results from the calculations are presented in section 4, and the conclusions from the study are discussed in section 5.

2. THEORY

In the eh-XCHF method,[79,80] the electron−hole wave function is represented by multiplying the mean-field wave function with an explicitly correlated function as shown in the following equation

$$\Psi_{\text{eh-XCHF}} = G\Phi^e\Phi^h \tag{5}$$

where Φ^e and Φ^h are electron and hole Slater determinants and G is a Gaussian-type geminal (GTG) function,[85] which is defined as

$$G(\mathbf{r}^e, \mathbf{r}^h) = \sum_{i=1}^{N_e}\sum_{j=1}^{N_h}\sum_{k=1}^{N_g} b_k \exp[-\gamma_k r_{ij}^2] \tag{6}$$

The GTG function depends on the r_{eh} term and is responsible for incorporating electron−hole interparticle distance dependence in the eh-XCHF wave function. The coefficients b_k and γ_k are expansion coefficients, which are obtained variationally. The Gaussian-type geminal functions have been used extensively in explicitly correlated methods for treating electron−electron correlation in many-electron systems.[86,87] They have also been used successfully for treating electron−hole correlation.[79,80] The use of Gaussian-type geminal functions offers three principle advantages. First, the variational determination of the geminal parameters $\{b_k,\gamma_k\}$ results in accurate description of the wave function near the electron−hole coalescence point. As can be seen in eq 4 the electron−hole recombination probability strongly depends on the form of the electron−hole wave function at small interparticle distances. Consequently, the use of Gaussian-type geminal functions and the variational determination of the geminal parameters are crucial for accurate computation of electron−hole recombination probability. The importance of the geminal function for the present work is highlighted in section 4.5. Second, the integrals of GTG functions with Gaussian-type orbitals (GTO) can be performed analytically and have been derived earlier by Boys[85] and Persson et al.[88] This alleviates the need to approximate the integrals using numerical methods. The third advantage of the GTG function is that it allows construction of a compact representation of an infinite-order configuration interaction expansion. This can be seen explicitly by introduction of the closure relationship

$$G|\Psi_{\text{ref}}\rangle = \underbrace{\sum_{ii'}^{\infty} |\Phi_i^e\Phi_{i'}^h\rangle\langle\Phi_i^e\Phi_{i'}^h|}_{\mathbf{1}} G|\Psi_{\text{ref}}\rangle. \tag{7}$$

The electron−hole interaction was described using the effective electron−hole Hamiltonian,[84,89−99] which is defined in the following equation

$$\begin{aligned} H = &\sum_{ij}\langle i|\frac{-\hbar^2}{2m_e} + v_{\text{ext}}^e|j\rangle e_i^\dagger e_j + \sum_{ij}\langle i|\frac{-\hbar^2}{2m_h} + v_{\text{ext}}^h|j\rangle h_i^\dagger h_j \\ &+ \sum_{iji'j'}\langle iji'j'|\varepsilon^{-1} r_{eh}^{-1}|iji'j'\rangle e_i^\dagger e_j h_{i'}^\dagger h_{j'} + \sum_{ijkl} w_{ijkl}^{ee} e_i^\dagger e_j^\dagger e_l e_k \\ &+ \sum_{ijkl} w_{ijkl}^{hh} h_i^\dagger h_j^\dagger h_l h_k \end{aligned} \tag{8}$$

The effective electron−hole Hamiltonian provides a computationally efficient route for investigating large systems and in the present work was used for investigating CdSe clusters in the range of $Cd_{20}Se_{19}$ to $Cd_{74608}Se_{74837}$. We have also developed eh-XCHF method using a pseudopotential,[100] but the current implementation is restricted to cluster sizes of 200 atoms and cannot be applied to large dot sizes.

The effective Hamiltonian in eq 8 was used in combination with parabolic potential which has been used extensively[101−110] for approximating the confining potential in quantum dots and wires. The electron and hole external potentials v_{ext}^{α} were expressed as

$$v_{\text{ext}}^{\alpha} = \frac{1}{2}k_{\alpha}|\mathbf{r}_{\alpha}|^2 \quad \alpha = \text{e, h} \tag{9}$$

The form of the external potential directly impacts the electron−hole pair density and is important for accurate computation of the binding energy and recombination probability. In this work, we have developed a particle number based search procedure for determining the external potential. The central idea of this method is to find an external potential such that the computed 1-particle electron and hole densities are spatially confined within the volume of the quantum dot. Mathematically, this is implemented by obtaining the force constant k by the following minimization process

$$\min_{k_{\alpha}^{\min}}(N_{\alpha} - \int_0^{D_{\text{dot}}/2} \mathrm{d}r^2 \int \mathrm{d}\Omega \rho_{\alpha}(\mathbf{r})[v_{\text{ext}}^{\alpha}])^2 \tag{10}$$

where α = e, h; $\mathrm{d}\Omega = \sin\theta\, \mathrm{d}\theta\, \mathrm{d}\phi$; D_{dot} is the dot diameter; and $k_{\alpha}^{\min}$ is the smallest force constant that satisfies the above minimization conditions. The single-particle density is a functional of the external potential and is denoted explicitly in the above equation.

The eh-XCHF wave function is obtained variationally by minimizing the eh-XCHF energy

$$E_{\text{eh-XCHF}} = \min_{G,\Phi^{\text{e}},\Phi^{\text{h}}} \frac{\langle \Psi_{\text{eh-XCHF}}|H|\Psi_{\text{eh-XCHF}}\rangle}{\langle \Psi_{\text{eh-XCHF}}|\Psi_{\text{eh-XCHF}}\rangle} \tag{11}$$

Instead of evaluating the above equation directly, it is more efficient to first transform the operators and then perform the integration over the coordinates. The transformed operators are obtained by performing congruent transformation,[111,112] which is defined as follows

$$\tilde{H} = G^{\dagger}HG \tag{12}$$

$$\tilde{1} = G^{\dagger}G \tag{13}$$

The eh-XCHF energy is obtained from the transformed operators using the following expression

$$E_{\text{eh-XCHF}} = \frac{\langle \Phi^{\text{e}}, \Phi^{\text{h}}|\tilde{H}|\Phi^{\text{e}}, \Phi^{\text{h}}\rangle}{\langle \Phi^{\text{e}}, \Phi^{\text{h}}|\tilde{1}|\Phi^{\text{e}}, \Phi^{\text{h}}\rangle} \tag{14}$$

The above equation allows us to reduce the minimization over the electron and hole Slater determinants in terms of coupled self-consistent field (SCF) equations as shown below[113]

$$\mathbf{F}_G^{\text{e}}[\mathbf{C}^{\text{h}}]\mathbf{C}^{\text{e}} = \lambda^{\text{e}}\mathbf{S}_G^{\text{e}}\mathbf{C}^{\text{e}} \tag{15}$$

$$\mathbf{F}_G^{\text{h}}[\mathbf{C}^{\text{e}}]\mathbf{C}^{\text{h}} = \lambda^{\text{h}}\mathbf{S}_G^{\text{h}}\mathbf{C}^{\text{h}} \tag{16}$$

This is identical to the Roothaan−Hall equation where $\mathbf{F}_G^{\text{e}}$ and $\mathbf{F}_G^{\text{e}}$ are Fock matrices for electron and holes, respectively. The subscript G in the above expression denotes that the Fock operators were obtained from the congruent transformed Hamiltonian and include contribution from the geminal operator. The functional form of the congruent transformed operators and the Fock operators have been derived earlier and can be found in ref 80. The single-particle basis for electrons and holes are constructed from the eigenfunctions of zeroth order single-particle Hamiltonian

$$H_0^{\alpha}\phi_i^{\alpha} = E_i^{\alpha}\phi_i^{\alpha} \quad \alpha = \text{e, h} \tag{17}$$

where the zeroth-order Hamiltonian is obtained from H using the following limiting condition

$$H_0 = H_0^{\text{e}} + H_0^{\text{h}} = \lim_{r_{\text{eh}}\to\infty} H \tag{18}$$

The exciton binding energy is computed using the following expression

$$E_{\text{EB}} = (E_0^{\text{e}} + E_0^{\text{h}}) - E_{\text{eh-XCHF}} \tag{19}$$

3. COMPUTATIONAL DETAILS

The material parameters for the CdSe quantum dots used in the electron−hole Hamiltonian in eq 8 were obtained from ref 91 and are presented in Table 1.The single-particle basis was constructed using a set of 10 s,p,d GTOs, as shown in eq 20

$$\phi = x^n y^m z^l \mathrm{e}^{-\alpha r^2} \tag{20}$$

The exponent of the GTOs and the force constants for the external potential used in the calculations are presented in Table 2. A set of three geminal functions were used for each dot size, where the geminal parameters were optimized variationally. The optimized parameters for all the dot sizes are presented in Table 3. The first set of geminal parameters were always set to $b_1 = 1$ and $\gamma_1 = 0$ to ensure that the eh-XCHF

Table 1. Material Parameters for the CdSe Quantum Dots Used in the Electron−Hole Hamiltonian

property	value (atomic units)[91]
m_{e}	0.13
m_{h}	0.38
ε	6.2

Table 2. Parameters for the External Potential and the GTOs Used in the eh-XCHF Calculation[a]

D_{dot} (nm)	k_{e}	k_{h}	α_{e}	α_{h}
1.24	2.66×10^{-2}	9.10×10^{-3}	2.94×10^{-2}	2.94×10^{-2}
1.79	6.22×10^{-3}	2.13×10^{-3}	1.42×10^{-2}	1.42×10^{-2}
2.76	1.10×10^{-3}	3.76×10^{-4}	5.98×10^{-3}	5.98×10^{-3}
2.98	8.10×10^{-4}	2.77×10^{-4}	5.13×10^{-3}	5.13×10^{-3}
3.28	5.52×10^{-4}	1.89×10^{-4}	4.24×10^{-3}	4.24×10^{-3}
3.79	3.09×10^{-4}	1.06×10^{-4}	3.17×10^{-3}	3.17×10^{-3}
4.80	1.20×10^{-4}	4.12×10^{-4}	1.98×10^{-3}	1.98×10^{-3}
6.60	3.38×10^{-5}	1.16×10^{-5}	1.05×10^{-3}	1.05×10^{-3}
10.0	6.41×10^{-6}	2.19×10^{-6}	4.57×10^{-4}	4.57×10^{-4}
15.0	1.26×10^{-6}	4.33×10^{-7}	2.03×10^{-4}	2.03×10^{-4}
20.0	4.01×10^{-7}	1.37×10^{-7}	1.14×10^{-4}	1.14×10^{-4}

[a]All values are given in atomic units.

dx.doi.org/10.1021/ct400485s | J. Chem. Theory Comput. 2013, 9, 4351−4359

Table 3. Optimized Geminal Parameters Obtained by Minimizing the eh-XCHF Energy[a]

D_{dot} (nm)	b_2	b_3	γ_2	γ_3
1.24	3.06	2.55×10^{-1}	1.40×10^{-3}	1.79×10^{-1}
1.79	2.16	2.69×10^{-1}	1.20×10^{-3}	9.80×10^{-2}
2.76	1.79	3.49×10^{-1}	9.00×10^{-4}	4.62×10^{-2}
2.98	1.69	3.50×10^{-1}	9.00×10^{-4}	4.21×10^{-2}
3.28	2.24	4.46×10^{-1}	7.00×10^{-4}	2.04×10^{-2}
3.79	1.98	4.56×10^{-1}	7.00×10^{-4}	2.01×10^{-2}
4.80	2.43	6.34×10^{-1}	6.00×10^{-4}	1.94×10^{-2}
6.60	2.43	8.05×10^{-1}	5.00×10^{-4}	1.71×10^{-2}
10.0	2.81	9.39×10^{-1}	5.00×10^{-4}	1.83×10^{-2}
15.0	3.35	1.29	4.00×10^{-4}	2.00×10^{-4}
20.0	3.27	1.38	2.00×10^{-4}	3.00×10^{-2}

[a]The first set of geminal parameters were set to $b_1 = 1$ and $g_1 = 0$ and the details are presented in the text. All values are given in atomic units.

energy is always bounded from above by the mean-field energy during the geminal optimization.[79,80]

4. RESULTS AND DISCUSSION

4.1. Exciton Binding Energy. The exciton binding energy was computed for a series of CdSe clusters ranging from $Cd_{20}Se_{19}$ to $Cd_{74608}Se_{74837}$. The approximate diameters of these quantum dots are in the range of 1 to 20 nm, respectively, and the results are presented in Table 4. It is seen that binding energy decreases as the size of the quantum dot increases. This trend is in agreement with earlier results.[32−34] In Figure 1, the computed binding energies are compared with previously reported experimental and theoretical results.[32−34,37−40] For D_{dot} equal to 1.8, 3.32, and 4.82 nm, Franceschetti and Zunger have computed binding energies using an atomistic pseudopotential based configuration interaction method,[32] and the exciton binding energies shown in Figure 1 were obtained from the tabulated values in ref 32. In a recent combined experimental and theoretical investigation, Jasieniak et al.[34] have reported size-dependent valence and conduction band energies of CdSe quantum dots. The values from the Jasieniak et al. studies in Figure 1 were obtained from the least-squares fit equation provided in ref 34. The remaining data points were obtained from the plot in ref 34. The log−log plot in Figure 1 shows that the computed binding energy is described very well by a linear-fit and the exciton binding energy scales as D^{-n} with respect to the dot size. This observation is consistent with the trend observed in earlier studies.[32−34] We find that the exciton binding energies from the eh-XCHF calculations are in very good agreement with the atomistic pseudopotential calculations by Wang et al.[37] and Franceschetti et al.[32] Comparing between eh-XCHF and Jasieniak et al.[34] results show that the eh-XCHF values are lower than the Jasieniak et al. values for small dot sizes, but the difference becomes smaller with increasing dot size. One possible explanation for this observation is that smaller quantum dots have high surface to volume ratios, and their optical properties are dominated by surface effects,[114,115] which are not currently included in the eh-XCHF calculations. The plot in Figure 1 highlights the ability of the eh-XCHF method to predict exciton binding energies for large quantum dots.

Table 4. Exciton Binding Energy Calculated Using eh-XCHF Method As Function of Dot Diameter

D_{dot} (nm)	Cd_xSe_y	E_{BE} (eV)
1.24	$Cd_{20}Se_{19}$	0.855
1.79	$Cd_{47}Se_{57}$	0.595
2.76	$Cd_{199}Se_{195}$	0.389
2.98	$Cd_{232}Se_{257}$	0.360
3.28	$Cd_{311}Se_{352}$	0.329
3.79	$Cd_{513}Se_{515}$	0.285
4.80	$Cd_{1012}Se_{1063}$	0.225
6.60	$Cd_{2704}Se_{2661}$	0.167
10.0	$Cd_{9338}Se_{9363}$	0.111
15.0	$Cd_{31534}Se_{31509}$	0.078
20.0	$Cd_{74608}Se_{74837}$	0.066

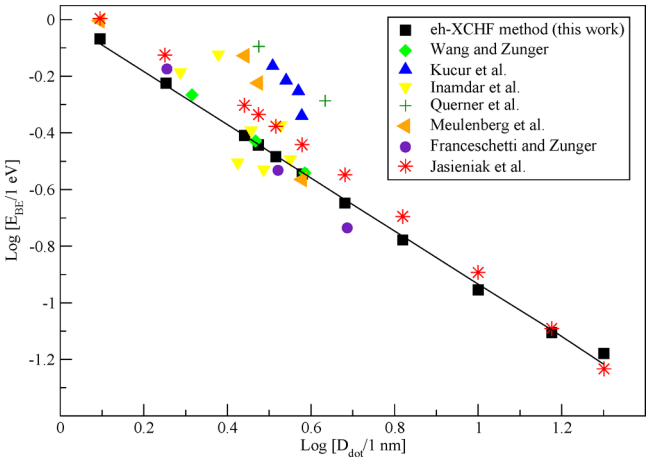

Figure 1. Log of binding energy (E_{BE}) versus log of diameter for CdSe quantum dots. The values from the eh-XCHF calculations are compared with results from earlier studies by Wang et al.,[37] Franceschetti et al.,[33] Meulenberg et al.,[32] Jasieniak et al.,[34] Kucur et al.,[38] Inamdar et al.,[39] and Querner et al.[40] The details of the comparison are presented in the text.

4.2. Electron−Hole Coulomb Energy. Another important quantity that is directly related to the electron−hole interaction is the electron−hole Coulomb energy. We have used the definition given by Franceschetti and Zunger[32] and calculated the electron−hole Coulomb energy using the following expression

$$A = \int d\mathbf{r}_e \, d\mathbf{r}_h \rho_{eh}(\mathbf{r}_e, \mathbf{r}_h) r_{eh}^{-1} \quad (21)$$

In Figure 2, we have compared the electron−hole Coulomb energy with the pseudopotential + CI calculations by Franceschetti and Zunger, and the results were found to be in good agreement with each other. The Coulomb energy is a very important quantity because it allows us to directly compare the quality of electron−hole pair density without introducing any additional approximation due to the choice of the dielectric function used for computation of the binding energy. The good agreement between the two methods provides important verification of the implementation of the eh-XCHF method.

4.3. Recombination Probability. In addition to exciton binding energies, electron−hole recombination probabilities were also calculated. Using the expression in eq 4, the electron−hole pair density from the eh-XCHF method was used in the computation of electron−hole recombination probabilities and the results are presented in Figure 3. A log−log plot of P_{eh} versus D_{dot} indicates that the recombination

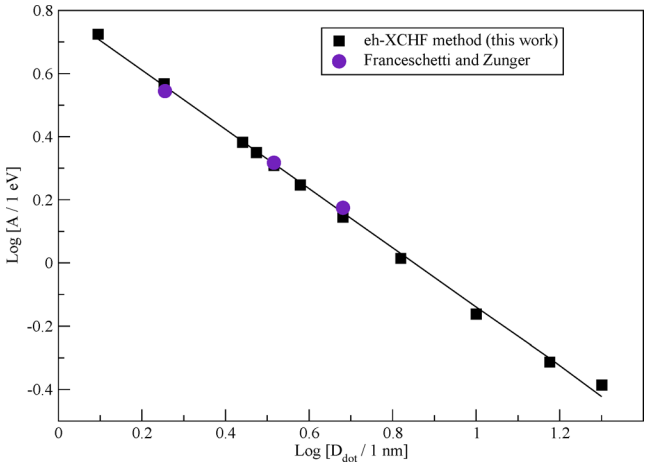

Figure 2. Log of Coulomb energy (A) for CdSe quantum dots versus log of diameter of quantum dot.

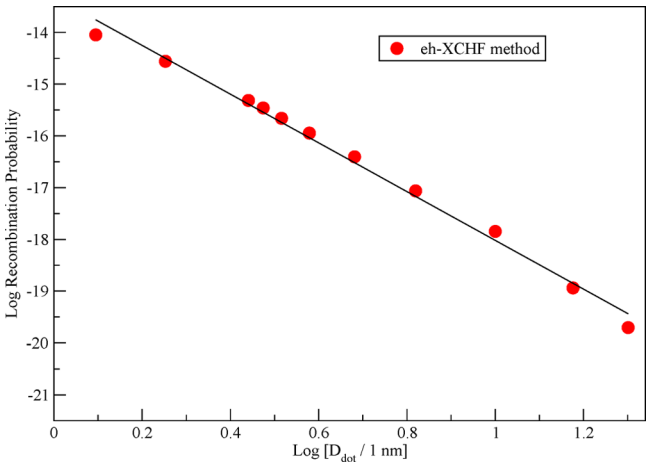

Figure 3. Log of recombination probability (P_{eh}) of CdSe quantum dots versus log of diameter of quantum dot.

probability also follows D_{dot}^{-n} dependence with dot diameter. One of the key results from this study is that the electron−hole recombination probability decreases at a much faster rate than the exciton binding energy with increasing dot size. This is illustrated in Figure 4, where comparison of the relative binding

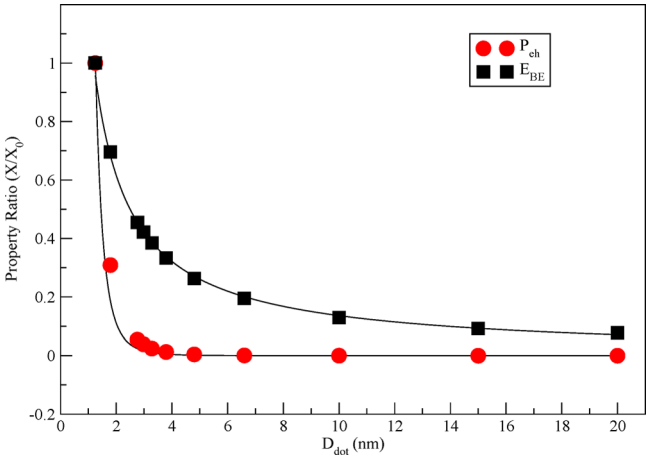

Figure 4. Comparison of E_{BE} and P_{eh} relative properties versus D_{dot}.

energy and recombination probability is presented with respect to dot size. We see that, at large dot sizes, both exciton binding energy and electron−hole recombination probability show weak dependence on the dot diameter D. This is consistent with the expected result that both of these quantities should become asymptotically invariant to the dot size. It was found that, for a factor of 16.1 change in the dot diameter, the exciton binding energy and the recombination probability decrease by a factor of 12.9 and 4.55×10^5, respectively.

The linear regression equations of the Coulomb energy, exciton binding energy, and electron−hole recombination probability as function of dot diameter are summarized in Table 5. It is seen that the slope for the recombination is

Table 5. Linear Regression Equation of Coulomb Energy, Exciton Binding Energy, and Electron−Hole Recombination Probability with Respect to Dot Diameter

property	equation
$\log[A/\text{eV}]$	$-0.938 \log[D/\text{nm}] + 0.7983$
$\log[E_{BE}/\text{eV}]$	$-0.938 \log[D/\text{nm}] + 0.0039$
$\log P_{eh}$	$-4.712 \log[D/\text{nm}] - 13.308$

substantially higher than the binding energy. The absolute value of the slope for both Coulomb energy and exciton binding energy was found to be lower than one which indicates that both of these quantities scale sublinearly with respect to D^{-1}. This is in contrast with the particle in a box model, which predicts a slope of −1. The sublinear scaling with respect to D^{-1} obtained in this work is in agreement with the previous results by Franceschetti et al.[33] and Meulenberg et al.,[32] respectively.

4.4. Effect of 1-Particle Basis Size. The convergence of the computed exciton binding energy and electron−hole recombination probability with respect to the size of the 1-particle basis was investigated by performing eh-XCHF calculation using two different sets of basis functions. The eh-XCHF calculations were performed using s and s, p, d GTOs and the results from the these calculations are summarized in Table 6. The change from s to s, p, d GTOs represents a 10-fold increase in the basis size for both electron and hole quasiparticles and it is seen from Table 6 that in all cases the change in the exciton binding energy is less than or equal to 5%. These results indicate that the exciton binding energies are converged with respect to the basis size. In contrast, the recombination probabilities were found to more sensitive to the

Table 6. Comparison of eh-XCHF Binding Energies and Recombination Probabilities Obtained Using s and s, p, d GTO Basis Functions

D_{dot} (nm)	$\%\Delta E_{BE}$	$\%\Delta P_{eh}$
1.24	1	3
1.79	1	5
2.76	1	7
2.98	2	8
3.28	2	9
3.79	2	10
4.80	3	14
6.60	3	15
10.0	5	21
15.0	4	7
20.0	2	33

dx.doi.org/10.1021/ct400485s | J. Chem. Theory Comput. 2013, 9, 4351−4359

change in the basis size and the maximum change in the P_{eh} was found to be 33%. Addition of another set of s,p,d, GTOs resulted in a maximum difference of 0.2% and 3% in the binding energy and recombination probability, respectively.

4.5. Comparison with Uncorrelated Wavfunction. In this section, the results from the eh-XCHF calculations are compared with the exciton binding energies and recombination probabilities obtained using the uncorrelated electron−hole wave function. The uncorrelated electron−hole wave function is a special case of the eh-XCHF wave function and can be obtained by setting the geminal correlation operator to $G = 1$ as shown in the following equation

$$\Psi_0 = \Phi_0^e \Phi_0^h \tag{22}$$

where Φ_0^α, α = e, h are eigen functions of the zeroth-order Hamiltonian H_0^α, α = e, h defined in eq 18. In order to evaluate the importance of the explicitly correlated ansatz, we define the following eh-XCHF wave function

$$\Psi_{\text{eh-XCHF}}{}' = G_{opt} \Phi_0^e \Phi_0^h \tag{23}$$

where the only difference between eq 22 and 23 is the presence of the G_{opt} term. The difference between the exciton binding energy and the recombination probability computed using the uncorrelated wave function and the eh-XCHF wave function in eq 23 are presented in Table 7.

Table 7. Comparison of Exciton Binding Energy and Recombination Probability Obtained Using the Uncorrelated Wavefunction and the eh-XCHF Method

D_{dot} (nm)	$\%\Delta E_{BE}$	$\%\Delta P_{eh}$
1.24	1	24
1.79	1	37
2.76	2	61
2.98	2	67
3.28	2	69
3.79	2	86
4.80	2	127
6.60	4	202
10.0	5	426
15.0	12	468
20.0	28	822

It is seen that, for small dots with diameters less than 5 nm, the computed exciton binding energies are in very good agreement with each other. The eh-XCHF exciton binding energy and the electron−hole recombination probability for the smallest three quantum dots were found to scale as $D^{-1.00}$ and $D^{-5.67}$, respectively. The scaling of exciton binding energy for the small dots is identical to the particle in a box result of D^{-1} and good agreement between the two methods indicate the dominance of the strong confinement effect in small quantum dots. However, in contrast to the binding energies, the corresponding errors in the recombination probabilities were found to be much higher. For larger quantum dots, it is seen that the uncorrelated wave function severely underestimates the electron−hole recombination probability. For the biggest quantum dots investigated in the present work, it was found the uncorrelated wave function underestimates the binding energy and recombination probability by 28% and 822%, respectively. The uncorrelated wave function is able to correctly predict that the recombination probability decreases at a faster rate than the binding energy with respect to size of the quantum dot. Specifically, increasing the dot size from 1.24 to 20 nm decreases the recombination probability obtained using the uncorrelated wave function by a factor of 1.7×10^7. However, this value was found to be higher by 2 orders of magnitude than the result of 4.6×10^5 obtained from the eh-XCHF calculation. Comparison between the two methods indicates that the accuracy of the uncorrelated wave function decreases significantly in the weak-confinement region. The results from Table 7 show the importance of explicitly correlated wave function for computation of electron−hole recombination probability and also highlight the limitation of using exciton binding energy as the sole criteria for characterizing the quality of the electron−hole wave function. This observation is also supported by previous study using path integral Monte Carlo (PIMC) method, where Wimmer and Shumway found that although both CI and PIMC gave comparable biexciton binding energies, the CI method can underestimate the recombination rates by a factor of 2.[91]

5. CONCLUSIONS

In conclusion, we have presented a multifaceted study of the effect of dot size on electron−hole interaction in CdSe quantum dots. The electron−hole explicitly correlated Hartree−Fock method was used for computation of exciton binding energy and electron−hole recombination probability. It was found that both exciton binding energy and electron−hole recombination probability decreases with increasing dot size and both quantities scale as D_{dot}^{-n} with respect to the diameter of the quantum dot. The computed exciton binding energies were found to be in good agreement with previously reported results. One of the significant results from these calculations is that the electron−hole recombination probability decreases at a substantially higher rate than the binding energy with increasing dot size. Changing the dot size by a factor of 16.1 resulted in a decrease in the electron−hole recombination probability by a factor of 10^5. Comparison of the explicitly correlated results with independent-particle approximation showed that the independent-particle approximation seriously underestimates the recombination probability at large dot sizes. For the 20 nm dot size, the error in exciton binding energy and electron−hole recombination probability computed using the independent-particle approximation were found to be 28% and 822%, respectively. The results from this study highlight the importance of electron−hole explicitly correlated wave function and also illustrate the limitations of using exciton binding energy as the sole metric for characterization of theoretical and computational methods.

AUTHOR INFORMATION

Corresponding Author

*E-mail: archakra@syr.edu.

Notes

The authors declare no competing financial interest.

ACKNOWLEDGMENTS

We thank professor Mathew Maye for insightful discussions, Christopher Blanton for assistance with graphics, and financial support from Syracuse University and the GAANN fellowship P200A090277 for this work.

REFERENCES

(1) Zhu, H.; Lian, T. Enhanced multiple exciton dissociation from CdSe quantum rods: The effect of nanocrystal shape. *J. Am. Chem. Soc.* **2012**, *134*, 11289−11297.

(2) Ghosh, Y.; Mangum, B. D.; Casson, J. L.; Williams, D. J.; Htoon, H.; Hollingsworth, J. A. New insights into the complexities of shell growth and the strong influence of particle volume in nonblinking "giant" core/shell nanocrystal quantum dots. *J. Am. Chem. Soc.* **2012**, *134*, 9634−9643.

(3) Bae, W. K.; Padilha, L. A.; Park, Y.-S.; McDaniel, H.; Robel, I.; Pietryga, J. M.; Klimov, V. I. Controlled alloying of the core/shell interface in CdSe/CdS quantum dots for suppression of auger recombination. *ACS Nano* **2013**, *7*, 3411−3419.

(4) Lin, Z.; Franceschetti, A.; Lusk, M. T. Size dependence of the multiple exciton generation rate in CdSe quantum dots. *ACS Nano* **2011**, *5*, 2503−2511.

(5) Alam, R.; Fontaine, D. M.; Branchini, B. R.; Maye, M. M. Designing quantum rods for optimized energy transfer with firefly luciferase enzymes. *Nano Lett.* **2012**, *12*, 3251−3256.

(6) Han, H.; Francesco, G. D.; Maye, M. M. Size control and photophysical properties of quantum dots prepared via a novel tunable hydrothermal route. *J. Phys. Chem. C* **2010**, *114*, 19270−19277.

(7) Williams, B. L.; Halliday, D. P.; Mendis, B. G.; Durose, K. Microstructure and point defects in CdTe nanowires for photovoltaic applications. *Nanotechnology* **2013**, *24*, 135703.

(8) Yin, J.; Yue, C.; Zang, Y.; Chiu, C.-H.; Li, J.; Kuo, H.-C.; Wu, Z.; Li, J.; Fang, Y.; Chen, C. Effect of the surface-plasmon−exciton coupling and charge transfer process on the photoluminescence of metal-semiconductor nanostructures. *Nanoscale* **2013**, *5*, 4436−4442.

(9) Jaeger, H. M.; Fischer, S.; Prezhdo, O. V. The role of surface defects in multi-exciton generation of lead selenide and silicon semiconductor quantum dots. *J. Chem. Phys.* **2012**, *136*, 064701.

(10) Kilina, S.; Velizhanin, K. A.; Ivanov, S.; Prezhdo, O. V.; Tretiak, S. Surface ligands increase photoexcitation relaxation rates in CdSe quantum dots. *ACS Nano* **2012**, *6*, 6515−6524.

(11) Kilina, S.; Ivanov, S.; Tretiak, S. Effect of surface ligands on optical and electronic spectra of semiconductor nanoclusters. *J. Am. Chem. Soc.* **2009**, *131*, 7717−7726.

(12) Kilina, S. V.; Kilin, D. S.; Prezhdo, O. V. Breaking the phonon bottleneck in PbSe and CdSe quantum dots: Time-domain density functional theory of charge carrier relaxation. *ACS Nano* **2009**, *3*, 93−99.

(13) Kelley, A. Electron−phonon coupling in CdSe nanocrystals. *J. Phys. Chem. Lett.* **2010**, *1*, 1296−1300.

(14) Kelley, A. Electron−-phonon coupling in CdSe nanocrystals from an atomistic phonon model. *ACS Nano* **2011**, *5*, 5254−5262.

(15) Kelley, A.; Dai, Q.; Jiang, Z.-j.; Baker, J.; Kelley, D. Resonance Raman spectra of wurtzite and zincblende CdSe nanocrystals. *Chem. Phys.* **2012**, *Article in press*.

(16) Kilina, S.; Kilin, D.; Prezhdo, V.; Prezhdo, O. Theoretical study of electron−phonon relaxation in PbSe and CdSe quantum dots: Evidence for phonon memory. *J. Phys. Chem. C* **2011**, *115*, 21641−21651.

(17) Hyeon-Deuk, K.; Prezhdo, O. Time-domain ab initio study of auger and phonon-assisted auger processes in a semiconductor quantum dot. *Nano Lett.* **2011**, *11*, 1845−1850.

(18) Hyeon-Deuk, K.; Prezhdo, O. Photoexcited electron and hole dynamics in semiconductor quantum dots: Phonon-induced relaxation, dephasing, multiple exciton generation, and recombination. *J. Phys.: Condens. Matter* **2012**, *24*, 363201.

(19) Kilina, S.; Neukirch, A.; Habenicht, B.; Kilin, D.; Prezhdo, O. Quantum zeno effect rationalizes the phonon bottleneck in semiconductor quantum dots. *Phys. Rev. Lett.* **2013**, *110*, 180404.

(20) Musa, I.; Massuyeau, F.; Cario, L.; Duvail, J. L.; Jobic, S.; Deniard, P.; Faulques, E. Temperature and size dependence of time-resolved exciton recombination in ZnO quantum dots. *Appl. Phys. Lett.* **2011**, *99*, 243107.

(21) Chon, B.; Bang, J.; Park, J.; Jeong, C.; Choi, J. H.; Lee, J.-B.; Joo, T.; Kim, S. Unique temperature dependence and blinking behavior of CdTe/CdSe (core/shell) type-II quantum dots. *J. Phys. Chem. C* **2011**, *115*, 436−442.

(22) Franceschetti, A.; Zunger, A. Exciton dissociation and interdot transport in CdSe quantum-dot molecules. *Phys. Rev. B* **2001**, *63*, 153304.

(23) Zhu, H.; Song, N.; Lian, T. Wave function engineering for ultrafast charge separation and slow charge recombination in type II core/shell quantum dots. *J. Am. Chem. Soc.* **2011**, *133*, 8762−8771.

(24) Zhu, H.; Song, N.; Lian, T. Controlling charge separation and recombination rates in CdSe/ZnS type I core/shell quantum dots by shell thicknesses. *J. Am. Chem. Soc.* **2010**, *132*, 15038−15045.

(25) Hoy, J.; Morrison, P. J.; Steinberg, L. K.; Buhro, W. E.; Loomis, R. A. Excitation energy dependence of the photoluminescence quantum yields of core and core/shell quantum dots. *J. Phys. Chem. C* **2013**, *4*, 2053−2060.

(26) Li, D.; Zhang, J.; Zhang, Q.; Xiong, Q. Electric-field-dependent photoconductivity in CdS nanowires and nanobelts: Exciton ionization, Franz−Keldysh, and Stark effects. *Nano Lett.* **2012**, *12*, 2993−2999.

(27) Yaacobi-Gross, N.; Soreni-Harari, M.; Zimin, M.; Kababya, S.; Schmidt, A.; Tessler, N. Molecular control of quantum-dot internal electric field and its application to CdSe-based solar cells. *Nat. Mater.* **2011**, *10*, 974−979.

(28) Liu, S.; Borys, N. J.; Huang, J.; Talapin, D. V.; Lupton, J. M. Exciton storage in CdSe/CdS tetrapod semiconductor nanocrystals: Electric field effects on exciton and multiexciton states. *Phys. Rev. B* **2012**, *86*, 045303.

(29) Perebeinos, V.; Avouris, P. Exciton ionization, Franz−Keldysh, and Stark effects in carbon nanotubes. *Nano Lett.* **2007**, *7*, 609−613.

(30) Blanton, C. J.; Brenon, C.; Chakraborty, A. Development of polaron-transformed explicitly correlated full configuration interaction method for investigation of quantum-confined Stark effect in GaAs quantum dots. *J. Chem. Phys.* **2013**, *138*, 054114.

(31) Park, K.; Deutsch, Z.; Li, J. J.; Oron, D.; Weiss, S. Single molecule quantum-confined stark effect measurements of semiconductor nanoparticles at room temperature. *ACS Nano* **2012**, *6*, 10013−10023.

(32) Franceschetti, A.; Zunger, A. Direct pseudopotential calculation of exciton coulomb and exchange energies in semiconductor quantum dots. *Phys. Rev. Lett.* **1997**, *78*, 915−918.

(33) Meulenberg, R. W.; Lee, J. R.; Wolcott, A.; Zhang, J. Z.; Terminello, L. J.; van Buuren, T. Determination of the exciton binding energy in CdSe quantum dots. *ACS Nano* **2009**, *3*, 325−330.

(34) Jasieniak, J.; Califano, M.; Watkins, S. E. Size-dependent valence and conduction band-edge energies of semiconductor nanocrystals. *ACS Nano* **2011**, *5*, 5888−5902.

(35) Maan, J. C.; Belle, G.; Fasolino, A.; Altarelli, M.; Ploog, K. Magneto-optical determination of exciton binding energy in GaAs−$Ga_{1-x}Al_xAs$ quantum wells. *Phys. Rev. B* **1984**, *30*, 2253−2256.

(36) Ramvall, P.; Tanaka, S.; Nomura, S.; Riblet, P.; Aoyagi, Y. Observation of confinement-dependent exciton binding energy of GaN quantum dots. *Appl. Phys. Lett.* **1998**, *73*, 1104−1106.

(37) Wang, L.-W.; Zunger, A. Pseudopotential calculations of nanoscale CdSe quantum dots. *Phys. Rev. B* **1996**, *53*, 9579−9582.

(38) Kucur, E.; Riegler, J.; Urban, G. A.; Nann, T. Determination of quantum confinement in CdSe nanocrystals by cyclic voltammetry. *J. Chem. Phys.* **2003**, *119*, 2333−2337.

(39) Inamdar, S. N.; Ingole, P. P.; Haram, S. K. Determination of band structure parameters and the quasi-particle gap of CdSe quantum dots by cyclic voltammetry. *ChemPhysChem* **2008**, *9*, 2574−2579.

(40) Querner, C.; Reiss, P.; Sadki, S.; Zagorska, M.; Pron, A. Size and ligand effects on the electrochemical and spectroelectrochemical responses of CdSe nanocrystals. *Phys. Chem. Chem. Phys.* **2005**, *7*, 3204−3209.

(41) García-Santamaría, F.; Chen, Y.; Vela, J.; Schaller, R. D.; Hollingsworth, J. A.; Klimov, V. I. Suppressed auger recombination in "giant" nanocrystals boosts optical gain performance. *Nano Lett.* **2009**, *9*, 3482−3488.

(42) Wang, L.-W.; Califano, M.; Zunger, A.; Franceschetti, A. Pseudopotential theory of auger processes in CdSe quantum dots. *Phys. Rev. Lett.* **2003**, *91*, 056404.
(43) Hyeon-Deuk, K.; Prezhdo, O. V. Multiple exciton generation and recombination dynamics in small Si and CdSe quantum dots: An ab initio time-domain study. *ACS Nano* **2012**, *6*, 1239−1250.
(44) Rabani, E.; Baer, R. Theory of multiexciton generation in semiconductor nanocrystals. *Chem. Phys. Lett.* **2010**, *496*, 227−235.
(45) Jaeger, H. M.; Hyeon-Deuk, K.; Prezhdo, O. V. Exciton multiplication from first principles. *Acc. Chem. Res.* **2013**, *46*, 1280−1289.
(46) Vela, J.; Htoon, H.; Chen, Y.; Park, Y.-S.; Ghosh, Y.; Goodwin, P. M.; Werner, J. H.; Wells, N. P.; Casson, J. L.; Hollingsworth, J. A. Effect of shell thickness and composition on blinking suppression and the blinking mechanism in "giant" CdSe/CdS nanocrystal quantum dots. *J. Biophoton.* **2010**, *3*, 706−717.
(47) Rawalekar, S.; Kaniyankandy, S.; Verma, S.; Ghosh, H. N. Ultrafast charge carrier relaxation and charge transfer dynamics of CdTe/CdS core/shell quantum dots as studied by femtosecond transient absorption spectroscopy. *J. Phys. Chem. C* **2010**, *114*, 1460−1466.
(48) Nemchinov, A.; Kirsanova, M.; Hewa-Kasakarage, N. N.; Zamkov, M. Synthesis and characterization of type II ZnSe/CdS core/shell nanocrystals. *J. Phys. Chem. C* **2008**, *112*, 9301−9307.
(49) Yan, Y.; Chen, G.; Van Patten, P. G. Ultrafast exciton dynamics in CdTe nanocrystals and core/shell CdTe/CdS nanocrystals. *J. Phys. Chem. C* **2011**, *115*, 22717−22728.
(50) Xu, Z.; Hine, C. R.; Maye, M. M.; Meng, Q.; Cotlet, M. Shell thickness dependent photoinduced hole transfer in hybrid conjugated polymer/quantum dot nanocomposites: From ensemble to single hybrid level. *ACS Nano* **2012**, *6*, 4984−4992.
(51) Noguchi, Y.; Sugino, O.; Nagaoka, M.; Ishii, S.; Ohno, K. A GWBethe-Salpeter calculation on photoabsorption spectra of (CdSe) 3 and (CdSe) 6 clusters. *J. Chem. Phys.* **2012**, *137*, 024306.
(52) Lopez Del Puerto, M.; Tiago, M.; Chelikowsky, J. Ab initio methods for the optical properties of CdSe clusters. *Phys. Rev. B* **2008**, *77*, 045404.
(53) Del Puerto, M.; Tiago, M.; Chelikowsky, J. Excitonic effects and optical properties of passivated CdSe clusters. *Phys. Rev. Lett.* **2006**, *97*, 096401.
(54) Nguyen, K.; Day, P.; Pachte. Understanding structural and optical properties of nanoscale CdSe magic-size quantum dots: Insight from computational prediction. *J. Phys. Chem. C* **2010**, *114*, 16197−16209.
(55) Yang, P.; Tretiak, S.; Ivanov, S. Influence of surfactants and charges on CdSe quantum dots. *J. Cluster Sci.* **2011**, *22*, 405−431.
(56) Albert, V.; Ivanov, S.; Tretiak, S.; Kilina, S. Electronic structure of ligated cdse clusters: Dependence on DFT methodology. *J. Phys. Chem. C* **2011**, *115*, 15793−15800.
(57) Kilin, D.; Tsemekhman, K.; Prezhdo, O.; Zenkevich, E.; von Borczyskowski, C. Ab initio study of exciton transfer dynamics from a core/shell semiconductor quantum dot to a porphyrin-sensitizer. *J. Photochem. Photobiol., A* **2007**, *190*, 342−351.
(58) Liu, C.; Chung, S.-Y.; Lee, S.; Weiss, S.; Neuhauser, D. Adsorbate-induced absorption redshift in an organic−inorganic cluster conjugate: Electronic effects of surfactants and organic adsorbates on the lowest excited states of a methanethiol−CdSe conjugate. *J. Chem. Phys.* **2009**, *131*, 174705.
(59) Chung, S.-Y.; Lee, S.; Liu, C.; Neuhauser, D. Structures and electronic spectra of CdSe−cys complexes: Density functional theory study of a simple peptide-coated nanocluster. *J. Phys. Chem. B* **2009**, *113*, 292−301.
(60) Kim, H.; Jang, S.-W.; Chung, S.; Lee, S.; Lee, Y.; Kim, B.; Liu, C.; Neuhauser, D. Effects of bioconjugation on the structures and electronic spectra of CdSe: Density functional theory study of CdSe−adenine complexes. *J. Phys. Chem. B* **2010**, *114*, 471−479.
(61) Nadler, R.; Sanz, J. Simulating the optical properties of CdSe clusters using the RT-TDDFT approach. *Theor. Chem. Acc.* **2013**, *132*, 1−9.
(62) Abuelela, A.; Mohamed, T.; Prezhdo, O. DFT simulation and vibrational analysis of the IR and Raman spectra of a CdSe quantum dot capped by methylamine and trimethylphosphine oxide ligands. *J. Phys. Chem. C* **2012**, *116*, 14674−14681.
(63) Fischer, S.; Crotty, A.; Kilina, S.; Ivanov, S.; Tretiak, S. Passivating ligand and solvent contributions to the electronic properties of semiconductor nanocrystals. *Nanoscale* **2012**, *4*, 904−914.
(64) Del Ben, M.; Havenith, R.; Broer, R.; Stener, M. Density functional study on the morphology and photoabsorption of CdSe nanoclusters. *J. Phys. Chem. C* **2011**, *115*, 16782−16796.
(65) Turkowski, V.; Leonardo, A.; Ullrich, C. Time-dependent density-functional approach for exciton binding energies. *Phys. Rev. B* **2009**, *79*, 233201.
(66) Li, Y.; Ullrich, C. Time-dependent transition density matrix. *Chem. Phys.* **2011**, *391*, 157−163.
(67) Yang, Z.-H.; Li, Y.; Ullrich, C. A minimal model for excitons within time-dependent density-functional theory. *J. Chem. Phys.* **2012**, *137*, 014513.
(68) Yang, Z.-H.; Ullrich, C. Direct calculation of exciton binding energies with time-dependent density-functional theory. *Phys. Rev. B* **2013**, *87*, 195204.
(69) Neuhauser, D.; Rabani, E.; Baer, R. Expeditious stochastic calculation of random-phase approximation energies for thousands of electrons in three dimensions. *J. Phys. Chem. Lett.* **2013**, *4*, 1172−1176.
(70) Franceschetti, A.; Fu, H.; Wang, L. W.; Zunger, A. Many-body pseudopotential theory of excitons in InP and CdSe quantum dots. *Phys. Rev. B* **1999**, *60*, 1819−1829.
(71) Baer, R.; Rabani, E. Communication: Biexciton generation rates in CdSe nanorods are length independent. *J. Chem. Phys.* **2013**, *138*, 051102.
(72) Rabani, E.; Hetenyi, B.; Berne, B. J.; Brus, L. E. Electronic properties of CdSe nanocrystals in the absence and presence of a dielectric medium. *J. Chem. Phys.* **1999**, *110*, 5355−5369.
(73) Wang, L.-W.; Zunger, A. Solving Schrödinger's equation around a desired energy: Application to silicon quantum dots. *J. Chem. Phys.* **1994**, *100*, 2394−2397.
(74) Canning, A.; Wang, L.; Williamson, A.; Zunger, A. Parallel empirical pseudopotential electronic structure calculations for million atom systems. *J. Comput. Phys.* **2000**, *160*, 29−41.
(75) Toledo, S.; Rabani, E. Verly large electronic structure calculations using an out-of-core filter-diagonalization method. *J. Comput. Phys.* **2002**, *180*, 256−269.
(76) Vömel, C.; Tomov, S.; Marques, O.; Canning, A.; Wang, L.-W.; Dongarra, J. State-of-the-art eigensolvers for electronic structure calculations of large scale nano-systems. *J. Comput. Phys.* **2008**, *227*, 7113−7124.
(77) Jordan, G.; Marsman, M.; Kim, Y.-S.; Kresse, G. Fast iterative interior eigensolver for millions of atoms. *J. Comput. Phys.* **2012**, *231*, 4836−4847.
(78) Mazziotti, D. *Advances in Chemical Physics, Reduced-Density-Matrix Mechanics: With Application to Many-Electron Atoms and Molecules*; Advances in Chemical Physics; Wiley: New York, 2007; p 574.
(79) Elward, J. M.; Thallinger, B.; Chakraborty, A. Calculation of electron-hole recombination probability using explicitly correlated Hartree−Fock method. *J. Chem. Phys.* **2012**, *136*, 124105.
(80) Elward, J. M.; Hoffman, J.; Chakraborty, A. Investigation of electron-hole correlation using explicitly correlated configuration interaction method. *Chem. Phys. Lett.* **2012**, *535*, 182−186.
(81) Wimmer, M.; Nair, S. V.; Shumway, J. Biexciton recombination rates in self-assembled quantum dots. *Phys. Rev. B* **2006**, *73*, 1−10.
(82) Cancio, A.; Chang, Y.-C. Quantum Monte Carlo study of polyexcitons in semiconductors. *Phys. Rev. B* **1990**, *42*, 11317−11324.
(83) Cancio, A.; Chang, Y.-C. Quantum Monte Carlo studies of binding energy and radiative lifetime of bound excitons in direct-gap semiconductors. *Phys. Rev. B* **1993**, *47*, 13246−13259.

(84) Zhu, X.; Hybertsen, M. S.; Littlewood, P. B. Electron-hole system revisited: A variational quantum Monte Carlo study. *Phys. Rev. B* **1996**, *54*, 13575−13580.
(85) Boys, S. F. The integral formulae for the variational solution of the molecular many-electron wave equations in terms of gaussian functions with direct electronic correlation. *Proc. R. Soc. A.* **1960**, *258*, 402−411.
(86) Kong, L.; Bischoff, F.; Valeev, E. Explicitly correlated R12/F12 methods for electronic structure. *Chem. Rev.* **2012**, *112*, 75−107.
(87) Höttig, C.; Klopper, W.; Köhn, A.; Tew, D. Explicitly correlated electrons in molecules. *Chem. Rev.* **2012**, *112*, 4−74.
(88) Persson, B. J.; Taylor, P. R. Accurate quantum-chemical calculations: The use of Gaussian-type geminal functions in the treatment of electron correlation. *J. Chem. Phys.* **1996**, *105*, 5915−5926.
(89) Hu, Y. Z.; Lindberg, M.; Koch, S. W. Theory of optically excited intrinsic semiconductor quantum dots. *Phys. Rev. B* **1990**, *42*, 1713−1723.
(90) Burovski, E. A.; Mishchenko, A. S.; Prokofév, N. V.; Svistunov, B. V. Diagrammatic quantum Monte Carlo for two-body problems: Applied to excitons. *Phys. Rev. Lett.* **2001**, *87*, 186402.
(91) Wimmer, M.; Nair, S. V.; Shumway, J. Biexciton recombination rates in self-assembled quantum dots. *Phys. Rev. B* **2006**, *73*, 165305.
(92) Woggon, U. *Optical Properties of Semiconductor Quantum Dots*; Springer Tracts in Modern Physics v. 136; Springer Verlag; Berlin, 1997; p 252.
(93) Braskén, M.; Lindberg, M.; Sundholm, D.; Olsen, J. Full configuration interaction calculations of electron-hole correlation effects in strain-induced quantum dots. *Phys. Status Solidi B* **2001**, *224*, 775−779.
(94) Corni, S.; Braskén, M.; Lindberg, M.; Olsen, J.; Sundholm, D. Stabilization energies of charged multiexciton complexes calculated at configuration interaction level. *Phys. E* **2003**, *18*, 436−442.
(95) Corni, S.; Braskén, M.; Lindberg, M.; Olsen, J.; Sundholm, D. Electron-hole recombination density matrices obtained from large configuration−interaction expansions. *Phys. Rev. B* **2003**, *67*, 853141−853147.
(96) Corni, S.; Braskén, M.; Lindberg, M.; Olsen, J.; Sundholm, D. Size dependence of the electron-hole recombination rates in semiconductor quantum dots. *Phys. Rev. B* **2003**, *67*, 453131−453139.
(97) Vänskä, T.; Lindberg, M.; Olsen, J.; Sundholm, D. Computational methods for studies of multiexciton complexes. *Phys. Status Solidi B* **2006**, *243*, 4035−4045.
(98) Vänskä, T.; Sundholm, D. Interpretation of the photoluminescence spectrum of double quantum rings. *Phys. Rev. B* **2010**, *82*, 085306.
(99) Sundholm, D.; Vänskä, T. Computational methods for studies of semiconductor quantum dots and rings. *Annu. Rep. Prog. Chem., Sect. C: Phys. Chem.* **2012**, *108*, 96−125.
(100) Elward, J. M.; Chakraborty, A. Atomistic pseudopotential calculation on CdSe quantum dots using electron-hole explicitly correlated Hartree−Fock method. (to be submitted).
(101) Halonen, V.; Chakraborty, T.; Pietiläinen, P. Excitons in a parabolic quantum dot in magnetic fields. *Phys. Rev. B* **1992**, *45*, 5980−5985.
(102) El-Said, M. Ground-state energy of an exciton in a parabolic quantum dot. *Semicond. Sci. Technol.* **1994**, *9*, 272−274.
(103) Jaziri, S.; Bennaceur, R. Excitons in parabolic quantum dots in electric and magnetic fields. *Semicond. Sci. Technol.* **1994**, *9*, 1775−1780.
(104) Lamouche, G.; Fishman, G. Two interacting electrons in a three-dimensional parabolic quantum dot: A simple solution. *J. Phys.: Condens. Matter* **1998**, *10*, 7857−7867.
(105) Xie, W.; Gu, J. Exciton bound to a neutral donor in parabolic quantum dots. *Phys. Lett. A* **2003**, *312*, 385−390.
(106) Xie, W. Exciton states trapped by a parabolic quantum dot. *Phys. B (Amsterdam, Neth.)* **2005**, *358*, 109−113.
(107) Xie, W. Effect of an electric field and nonlinear optical rectification of confined excitons in quantum dots. *Phys. Status Solidi B* **2009**, *246*, 2257−2262.
(108) Karimi, M.; Rezaei, G. Effects of external electric and magnetic fields on the linear and nonlinear intersubband optical properties of finite semi-parabolic quantum dots. *Phys. B (Amsterdam, Neth.)* **2011**, *406*, 4423−4428.
(109) Nammas, F.; Sandouqa, A.; Ghassib, H.; Al-Sugheir, M. Thermodynamic properties of two-dimensional few-electrons quantum dot using the static fluctuation approximation (SFA). *Phys. B (Amsterdam, Neth.)* **2011**, *406*, 4671−4677.
(110) Rezaei, G.; Vaseghi, B.; Sadri, M. External electric field effect on the optical rectification coefficient of an exciton in a spherical parabolic quantum dot. *Phys. B (Amsterdam, Neth.)* **2011**, *406*, 4596−4599.
(111) Elward, J. M.; Hoja, J.; Chakraborty, A. Variational solution of the congruently transformed Hamiltonian for many-electron systems using a full-configuration-interaction calculation. *Phys. Rev. A* **2012**, *86*, 062504.
(112) Bayne, M.; Drogo, J.; Chakraborty, A. Infinite-order diagrammatic summation approach to explicitly correlated congruent transformed Hamiltonian. arXiv preprint arXiv:1306.2446, 2013.
(113) Swalina, C.; Pak, M. V.; Chakraborty, A.; Hammes-Schiffer, S. Explicit dynamical electron−proton correlation in the nuclear−electronic orbital framework. *J. Phys. Chem. A* **2006**, *110*, 9983−9987.
(114) Jasieniak, J.; Mulvaney, P. From Cd-rich to Se-rich—The manipulation of CdSe nanocrystal surface stoichiometry. *J. Am. Chem. Soc.* **2007**, *129*, 2841−2848.
(115) Luther, J. M.; Pietryga, J. M. Stoichiometry control in quantum dots: A viable analog to impurity doping of bulk materials. *ACS Nano* **2013**, *7*, 1845−1849.